

Superpartner mass measurements with 1D decomposed M_{T2}

Partha Konar¹, Kyoungchul Kong², Konstantin T. Matchev¹, and Myeonghun Park¹

¹*Physics Department, University of Florida, Gainesville, FL 32611, USA* and

²*Theoretical Physics Department, SLAC, Menlo Park, CA 94025*

(Dated: 19 March, 2010)

We propose a new model-independent technique for mass measurements in missing energy events at hadron colliders. We illustrate our method with the most challenging case of a short, single-step decay chain. We consider inclusive same-sign chargino pair production in supersymmetry, followed by leptonic decays to sneutrinos: $\chi^+ \chi^+ \rightarrow \ell^+ \ell^+ \tilde{\nu}_\ell \tilde{\nu}_{\ell'} (\chi^- \chi^- \rightarrow \ell^- \ell^- \tilde{\nu}_\ell^* \tilde{\nu}_{\ell'}^*)$. We introduce two one-dimensional decompositions of the Cambridge M_{T2} variable: $M_{T2\parallel}$ and $M_{T2\perp}$, on the direction of the upstream transverse momentum \vec{P}_T and the direction orthogonal to it, respectively. We show that the sneutrino mass M_c can be measured directly by minimizing the number of events $N(\tilde{M}_c)$ in which M_{T2} exceeds a certain threshold, conveniently measured from the endpoint $M_{T2\perp}^{max}(\tilde{M}_c)$.

PACS numbers: 14.80.Ly, 12.60.Jv, 11.80.Cr

The Large Hadron Collider (LHC) at CERN has begun its long awaited exploration of the TeV scale, where new physics beyond the Standard Model (SM) may hold the key to our understanding of some very basic questions about our universe: What is the dark matter? What are the fundamental symmetries of Nature? Are there any hidden dimensions of space? A potential discovery of a missing energy signal at the LHC may relate to all three of these questions, if the missing energy is due to a stable, neutral, weakly interacting massive particle in a theory with space-time supersymmetry (SUSY) [1] or extra dimensions [2].

The first order of business after the discovery of a missing energy signal at the LHC will be to measure the mass of the missing particle and prove that it is not simply a SM neutrino [3]. This deceptively simple task turned out to be a notoriously difficult challenge. The generic topology of a prototypical “SUSY-like” missing energy event is schematically depicted in Fig. 1. Consider inclusive production of an identical pair of new particles P (from now on referred to as “parents”). Each parent decays semi-invisibly to a set of SM particles V_i , ($i = 1, 2$), which are visible in the detector, and a dark matter particle C (from now on referred to as the “child”) which escapes detection. In general, the parent pair may be accompanied by a number of additional “upstream” objects U (typically jets) with total transverse momentum \vec{P}_T . They may originate from various sources such as initial state radiation or decays of even heavier particles up the decay chain. We shall not be interested in the exact details of the physics responsible for U , adopting a fully inclusive approach to the production of the parents P . Given this general setup, the goal is to determine *independently* the mass M_p of the parent and the mass M_c of the child.

In the past, several approaches to this problem have been proposed, e.g. invariant mass endpoint measurements [4] or exact reconstruction of the missing particle momenta \vec{p}_{iT}^c [5]. Unfortunately, they only apply to sufficiently long decay chains, where the visible particles in V_i arise from a sequence of at least three 2-body decays

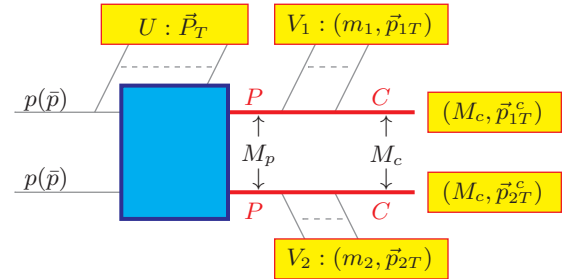


FIG. 1: The generic event topology under consideration. All particles visible in the detector are clustered into three groups: upstream objects U with total transverse momentum \vec{P}_T , and two composite visible particles V_i , each with invariant mass m_i and total transverse momentum \vec{p}_{iT} . The transverse momenta of the two missing particles are labelled by \vec{p}_{iT}^c .

[6]. In the simplest example of a short, single-step decay chain, each V_i consists of a single SM particle of fixed mass m_i , and neither of these two approaches will work. One must then resort to methods based on the Cambridge M_{T2} variable [7–9] or the related Sheffield M_{CT} variable [10, 11]. Unfortunately, in order to apply those techniques, one must work with a subset of events within a relatively narrow fixed P_T range, incurring some loss in statistics.

In this Letter we propose a new method which uses the full data set, with no such loss in statistics. Our method is based on the “subsystem” variant [9] of the original M_{T2} variable [7]. For any given event, one can construct the transverse mass M_{iT} of each parent P :

$$M_{iT}^2 \equiv m_i^2 + M_c^2 + 2(E_{iT}E_{iT}^c - \vec{p}_{iT} \cdot \vec{p}_{iT}^c), \quad (1)$$

where

$$E_{iT} \equiv \sqrt{m_i^2 + |\vec{p}_{iT}|^2}, \quad E_{iT}^c \equiv \sqrt{M_c^2 + |\vec{p}_{iT}^c|^2}, \quad (2)$$

is the transverse energy of the visible particle V_i and child particle C in each branch of Fig. 1, correspondingly. The individual momenta \vec{p}_{iT}^c of the missing child particles C

are unknown, but they are constrained by the measured missing transverse momentum \vec{P}_T in the event:

$$\vec{p}_{1T}^c + \vec{p}_{2T}^c = \vec{P}_T \equiv -\vec{P}_T - \vec{p}_{1T} - \vec{p}_{2T}. \quad (3)$$

For the true values of the missing momenta \vec{p}_{iT}^c , each transverse mass in (1) is bounded from above by the true parent mass M_P . This fact can be used in a rather ingenious way to define the Cambridge M_{T2} variable [7]. One takes the larger of the two quantities in (1) and minimizes it over all possible partitions of the unknown children momenta \vec{p}_{iT}^c , subject to the constraint (3):

$$M_{T2} \equiv \min_{\vec{p}_{1T}^c + \vec{p}_{2T}^c = \vec{P}_T} \{\max \{M_{1T}, M_{2T}\}\}. \quad (4)$$

For a given P_T , the endpoint M_{T2}^{max} of this distribution gives the parent mass \tilde{M}_p as a function of the input trial child mass \tilde{M}_c :

$$\tilde{M}_p(\tilde{M}_c, P_T) \equiv M_{T2}^{max}(\tilde{M}_c, P_T). \quad (5)$$

This property provides one relation among the two unknown masses M_p and M_c [7].

Here we propose to obtain a second relation by using the property that the function $\tilde{M}_p(\tilde{M}_c, P_T)$ is independent of P_T at the true child mass M_c :

$$\tilde{M}_p(M_c, P_T + \Delta P_T) - \tilde{M}_p(M_c, P_T) = 0, \forall \Delta P_T, \quad (6)$$

which we can rewrite more informatively as

$$\tilde{M}_p(\tilde{M}_c, P_T) - \tilde{M}_p(\tilde{M}_c, 0) \geq 0, \quad (7)$$

with equality being achieved only for $\tilde{M}_c = M_c$. Eq. (7) implies that, for any given \tilde{M}_c , there will always be a certain number of events whose M_{T2} values will exceed the reference value $\tilde{M}_p(\tilde{M}_c, 0)$, unless the trial mass \tilde{M}_c happens to coincide with the true child mass M_c . In order to quantify this effect, we define the function

$$N(\tilde{M}_c) \equiv \sum_{\text{all events}} H(M_{T2} - \tilde{M}_p(\tilde{M}_c, 0)), \quad (8)$$

where $H(x)$ is the Heaviside step function. From the definition of $N(\tilde{M}_c)$ it is clear that it is minimized at $\tilde{M}_c = M_c$, where in theory we would expect

$$N_{min} \equiv \min\{N(\tilde{M}_c)\} = N(M_c) = 0. \quad (9)$$

In reality, the value of N_{min} will be lifted from 0, due to finite particle width effects, detector resolution, etc. Nevertheless we expect that the *location* of the $N(\tilde{M}_c)$ minimum will still be at $\tilde{M}_c = M_c$, allowing a direct measurement of the child mass M_c :

$$M_c = \left\{ \tilde{M}_c \mid N(\tilde{M}_c) = N_{min} \right\}, \quad (10)$$

which is our first main result. Once the child mass M_c is found from (10), the true parent mass M_p is obtained as usual from (5) as $M_p = \tilde{M}_p(M_c, P_T)$.

At this point it is not clear whether we have gained anything statistics-wise, since the reference quantity $\tilde{M}_p(\tilde{M}_c, 0)$ appearing in the definition (8) has to be measured at a fixed $P_T = 0$ anyway. Our second main result in this paper is that $\tilde{M}_p(\tilde{M}_c, 0)$ can in fact be measured from the full data set with no loss in statistics as follows.

Let us introduce one-dimensional (1D) decompositions of M_{T2} onto the two special directions defined by the upstream momentum vector \vec{P}_T . Following Ref. [11], first project the visible transverse momenta \vec{p}_{iT} of Fig. 1 onto the \vec{P}_T direction ($T_{||}$) and its orthogonal direction (T_{\perp}):

$$\vec{p}_{iT_{||}} \equiv \frac{1}{P_T^2} (\vec{p}_{iT} \cdot \vec{P}_T) \vec{P}_T, \quad (11)$$

$$\vec{p}_{iT_{\perp}} \equiv \vec{p}_{iT} - \vec{p}_{iT_{||}} = \frac{1}{P_T^2} \vec{P}_T \times (\vec{p}_{iT} \times \vec{P}_T), \quad (12)$$

and similarly for the two transverse momenta \vec{p}_{iT}^c of the children and for \vec{P}_T . Now consider the corresponding 1D decompositions of the transverse parent masses (1)

$$E_{iT_{||}}^2 \equiv m_i^2 + \tilde{M}_c^2 + 2(E_{iT_{||}} E_{iT_{||}}^c - \vec{p}_{iT_{||}} \cdot \vec{p}_{iT_{||}}^c),$$

$$E_{iT_{\perp}}^2 \equiv m_i^2 + \tilde{M}_c^2 + 2(E_{iT_{\perp}} E_{iT_{\perp}}^c - \vec{p}_{iT_{\perp}} \cdot \vec{p}_{iT_{\perp}}^c),$$

in terms of the 1D projected analogues of (2)

$$E_{iT_{||}} \equiv \sqrt{m_i^2 + |\vec{p}_{iT_{||}}|^2}, \quad E_{iT_{\perp}} \equiv \sqrt{m_i^2 + |\vec{p}_{iT_{\perp}}|^2},$$

$$E_{iT_{||}}^c \equiv \sqrt{\tilde{M}_c^2 + |\vec{p}_{iT_{||}}^c|^2}, \quad E_{iT_{\perp}}^c \equiv \sqrt{\tilde{M}_c^2 + |\vec{p}_{iT_{\perp}}^c|^2}.$$

Now we define 1D M_{T2} decompositions in complete analogy with the standard M_{T2} definition (4):

$$M_{T2_{||}} \equiv \min_{\vec{p}_{1T_{||}}^c + \vec{p}_{2T_{||}}^c = \vec{P}_{T_{||}}} \{\max \{M_{1T_{||}}, M_{2T_{||}}\}\}, \quad (13)$$

$$M_{T2_{\perp}} \equiv \min_{\vec{p}_{1T_{\perp}}^c + \vec{p}_{2T_{\perp}}^c = \vec{P}_{T_{\perp}}} \{\max \{M_{1T_{\perp}}, M_{2T_{\perp}}\}\}. \quad (14)$$

These decompositions are extremely useful. For once, the 1D variables (13,14) can be calculated via simple analytic expressions as shown below. In contrast, a general formula for the original M_{T2} variable (4) in the presence of arbitrary P_T is unknown and one still has to compute M_{T2} numerically [12]. More importantly, $M_{T2_{\perp}}$ allows us to measure the reference quantity $\tilde{M}_p(\tilde{M}_c, 0)$ in (8) from the full data set, using events with *any* value of P_T .

To understand the basic idea, it is sufficient to consider the simplest, yet most challenging case of a single step decay chain. Let V_i be a single, (approximately) massless SM particle: $m_1 = m_2 = 0$. (The discussion for the massive case proceeds analogously.) In what follows, for illustration we shall use the same-sign dilepton channel in supersymmetry, where each V_i is a lepton resulting from a chargino decay to a sneutrino [9]. The charginos themselves are produced indirectly in the decays of squarks and gluinos. For concreteness we shall use a SUSY spectrum given by the LM6 CMS study point [13]. At point

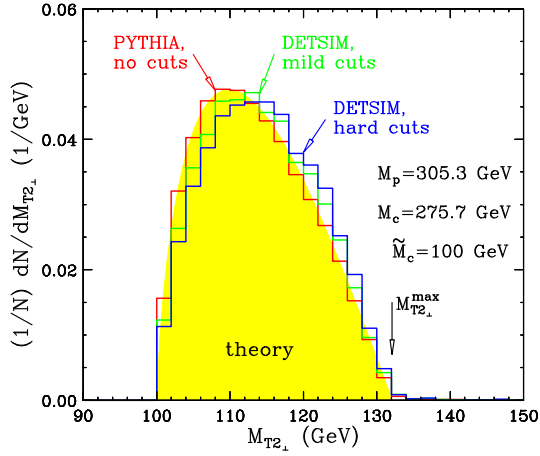


FIG. 2: The unit-normalized $M_{T2\perp}$ distribution (19) for the same-sign dilepton channel in a SUSY model with LM6 CMS mass spectrum and a choice of test mass $\tilde{M}_c = 100$ GeV. The yellow shaded distribution shows the theoretically predicted shape (19), matching very well the parton level result from PYTHIA with no cuts (red histogram). The green (blue) histogram is the corresponding result after PGS detector simulation with mild (hard) cuts as explained in the text. The endpoint expected from eq. (16) is 132.1 GeV and is marked with the vertical arrow.

LM6, the chargino (sneutrino) mass is $M_p = 305.3$ GeV ($M_c = 275.7$ GeV), and the rest of the SUSY mass spectrum can be found in [13]. In our simulations we use the PYTHIA event generator [14] and the PGS detector simulation program [15].

The variable $M_{T2\perp}$ has several unique properties. Eventwise, it can be calculated analytically as

$$M_{T2\perp} = \sqrt{A_{T\perp}} + \sqrt{A_{T\perp} + \tilde{M}_c^2}, \quad (15)$$

$$A_{T\perp} \equiv \frac{1}{2} (\vec{p}_{1T\perp} \cdot \vec{p}_{2T\perp}).$$

The endpoint of the $M_{T2\perp}$ distribution is given by

$$M_{T2\perp}^{max}(\tilde{M}_c) = \mu + \sqrt{\mu^2 + \tilde{M}_c^2}, \quad (16)$$

in terms of the parameter μ introduced in [6]

$$\mu \equiv \frac{M_p}{2} \left(1 - \frac{M_c^2}{M_p^2} \right). \quad (17)$$

Eq. (16) reveals perhaps the most important feature of the $M_{T2\perp}$ variable: its endpoint is *independent* of the upstream P_T and can thus be measured with the *whole* event sample. We can even predict analytically the *shape* of the (unit-normalized) differential $M_{T2\perp}$ distribution

$$\frac{dN}{dM_{T2\perp}} = N_{0\perp} \delta(M_{T2\perp} - \tilde{M}_c) + (1 - N_{0\perp}) \frac{d\bar{N}}{dM_{T2\perp}}, \quad (18)$$

where $N_{0\perp}$ is the fraction of events in the lowest \tilde{M}_c bin

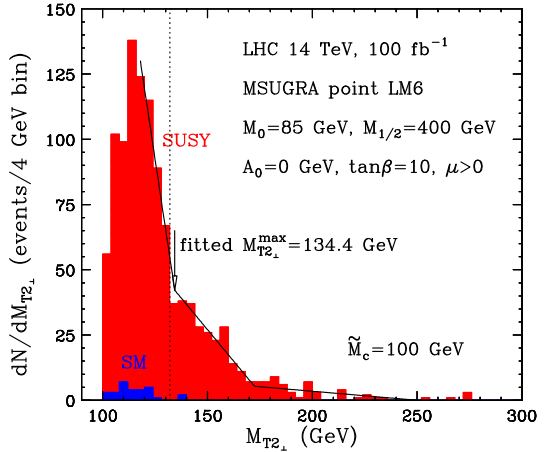


FIG. 3: Observable $M_{T2\perp}$ distribution after hard cuts for 100 fb^{-1} of LHC data. The total stacked distribution consists of the SUSY signal (red) and the SM background (blue). The solid line is the result of a simple linear fit, revealing endpoints at 134.4 GeV and 172.4 GeV.

$M_{T2\perp} = \tilde{M}_c$, while the shape of the remaining (unit-normalized) $M_{T2\perp}$ distribution is given by (see Fig. 2)

$$\frac{d\bar{N}}{dM_{T2\perp}} = \frac{M_{T2\perp}^4 - \tilde{M}_c^4}{\mu^2 M_{T2\perp}^3} \ln \left(\frac{2\mu M_{T2\perp}}{M_{T2\perp}^2 - \tilde{M}_c^2} \right). \quad (19)$$

Notice that this shape does not depend on any unknown kinematic parameters, such as the unknown center-of-mass energy or longitudinal momentum of the initial hard scattering. It is also insensitive to spin correlation effects, whenever the upstream momentum results from production and/or decay processes involving scalar particles (e.g. squarks) or vectorlike couplings (e.g. the QCD gauge coupling). It is even independent of the actual value of the upstream momentum P_T . Thus we are not restricted to a particular P_T range and can use the *whole* event sample in the $M_{T2\perp}$ analysis. For any choice of \tilde{M}_c (in Fig. 2 we used $\tilde{M}_c = 100$ GeV), eq. (19) is a one-parameter curve which can be fitted to the data to obtain the parameter μ and from there the $M_{T2\perp}$ endpoint (16).

As always, there are practical limitations to the use of such shape fitting. First, the shape (19) is modified in the presence of “mild” cuts, which are required for lepton identification in PGS (green histogram in Fig. 2), and more importantly, for the discovery of the same-sign dilepton SUSY signal over the SM backgrounds. To ensure discovery, we use “hard” cuts as follows [13, 16]: exactly two isolated leptons with $p_T > 10$ GeV, at least three jets with $p_T > (175, 130, 55)$ GeV, $\cancel{P}_T > 200$ GeV and a veto on tau jets. With those cuts, in the dimuon channel alone, the remaining SM background cross-section is dominated by $t\bar{t}$ and is just 0.15 fb, while the SUSY signal is 14 fb, leading to a 22σ discovery with just 10 fb^{-1} of data [13, 16]. The distortion of the $M_{T2\perp}$ shape with these hard offline cuts is illustrated by the blue (rightmost) histogram in Fig. 2. The actual $M_{T2\perp}$

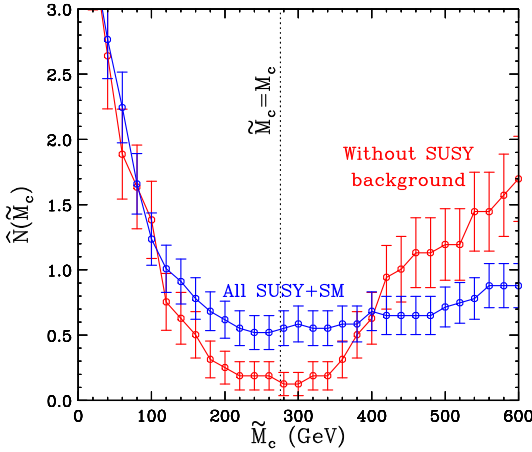


FIG. 4: The function $\hat{N}(\tilde{M}_c)$ defined in (22). The blue (red) set of measurements are with (without) SUSY combinatorial background. The error bars shown are purely statistical.

distribution which we expect to observe with 100 fb^{-1} of data, is shown in Fig. 3 and is comprised of a relatively small SM background component (blue) and a dominant SUSY signal component (red). In spite of the presence of a sizable SUSY combinatorial background, the $M_{T2\perp}$ endpoint expected from Fig. 2 is clearly visible and its location from a simple linear fit is obtained as 134.4 GeV, which is very close to the nominal value of 132.1 GeV. (Interestingly, the data reveals a second endpoint at 172.4 GeV, which is due to events in which one chargino decays through a charged slepton: $\tilde{\chi}_1^\pm \rightarrow \tilde{\ell}_L^\pm \rightarrow \tilde{\chi}_1^0$ [9]. Its nominal value is 169.2 GeV.)

Our final key observation is that

$$\tilde{M}_p(\tilde{M}_c, 0) = M_{T2}^{\max}(\tilde{M}_c, 0) = M_{T2\perp}^{\max}(\tilde{M}_c), \quad (20)$$

which allows to rewrite the function $N(\tilde{M}_c)$ of eq. (8) as

$$N(\tilde{M}_c) \equiv \sum_{\text{all events}} H\left(M_{T2} - M_{T2\perp}^{\max}(\tilde{M}_c)\right). \quad (21)$$

The $M_{T2\perp}$ analysis just described allows a very pre-

cise measurement of the benchmark quantity $M_{T2\perp}^{\max}(\tilde{M}_c)$ appearing in (21), so that the function $N(\tilde{M}_c)$ itself can be reliably reconstructed, using *the whole event sample* all the way throughout the analysis, without any loss in statistics. We show our result in Fig. 4, where for convenience we unit-normalize the function $N(\tilde{M}_c)$ as

$$\hat{N}(\tilde{M}_c) = N(\tilde{M}_c)/\langle N(\tilde{M}_c) \rangle, \quad (22)$$

where the averaging is performed over the plotted range of \tilde{M}_c . As expected, the function $\hat{N}(\tilde{M}_c)$ exhibits a minimum in the vicinity of the true sneutrino mass $\tilde{M}_c = M_c = 275.7 \text{ GeV}$. Ignoring the SUSY combinatorial background, this measurement (red data points) is quite precise, at the level of a few percent. In order to reduce the combinatorial background, we select events with $\tilde{M}_c < M_{T2\perp} < M_{T2\perp}^{\max}$ and veto very hard[17] leptons with $p_T > 60 \text{ GeV}$. The resulting M_c measurement (blue data points) is at the level of 10%. This precision is clearly sufficient to exclude SM neutrinos as the source of the missing energy, hinting at a potential dark matter discovery at the LHC.

In conclusion, we summarize the novel features and advantages of our method in comparison to previous M_{T2} -based proposals in the literature [8, 9]. First, we make crucial use of property (6), which allowed us to measure *directly* the missing particle mass M_c as in eq. (10). Second, both the benchmark quantity $M_{T2\perp}^{\max}(M_c)$ entering eq. (21) as well as the the function $N(\tilde{M}_c)$ itself can be measured using the whole available data sample at *any* P_T . To the extent that the definition of $M_{T2\perp}$ relies only on the *direction* and not the magnitude of the upstream \vec{P}_T , our method is insensitive to the jet energy scale error [11]. We have also provided exact analytical formulas for the computation of the 1D decomposed M_{T2} variables[18] and the shape (19) of the $M_{T2\perp}$ distribution.

Acknowledgments. We thank L. Pape for useful comments. This work is supported in part by US Department of Energy grants DE-FG02-97ER41029 and DE-AC02-76SF00515.

[1] See, e.g. D. Chung *et al.*, Phys. Rept. **407**, 1 (2005).
[2] D. Hooper and S. Profumo, Phys. Rept. **453**, 29 (2007).
[3] S. Chang and A. de Gouvea, Phys. Rev. D **80**, 015008 (2009).
[4] I. Hinchliffe *et al.*, Phys. Rev. D **55**, 5520 (1997); B. C. Allanach, C. G. Lester, M. A. Parker and B. R. Webber, JHEP **0009**, 004 (2000); B. K. Gjelsten, D. J. Miller and P. Oslund, JHEP **0412**, 003 (2004); D. Costanzo and D. R. Tovey, JHEP **0904**, 084 (2009); M. Burns, K. T. Matchev and M. Park, JHEP **0905**, 094 (2009); K. T. Matchev, F. Moortgat, L. Pape and M. Park, JHEP **0908**, 104 (2009).
[5] K. Kawagoe, M. Nojiri and G. Polesello, Phys. Rev. D **71**, 035008 (2005); H. C. Cheng *et al.*, JHEP **0712**, 076 (2007); M. Nojiri, G. Polesello and D. R. Tovey, JHEP **0805**, 014 (2008); H. C. Cheng *et al.*, Phys. Rev. Lett. **100**, 252001 (2008); B. Webber, JHEP **0909**, 124 (2009).
[6] M. Burns, K. Kong, K. T. Matchev and M. Park, JHEP **0903**, 143 (2009).
[7] C. Lester and D. Summers, Phys. Lett. B **463**, 99 (1999); A. Barr, C. Lester and P. Stephens, J. Phys. G **29**, 2343 (2003).
[8] W. Cho, K. Choi, Y. Kim and C. Park, Phys. Rev. Lett. **100**, 171801 (2008); JHEP **0802**, 035 (2008); B. Gripaios, JHEP **0802**, 053 (2008); A. Barr, B. Gripaios and C. Lester, JHEP **0802**, 014 (2008).

- [9] K. T. Matchev, F. Moortgat, L. Pape and M. Park, arXiv:0909.4300 [hep-ph].
- [10] D. R. Tovey, JHEP **0804**, 034 (2008); G. Polesello and D. R. Tovey, arXiv:0910.0174 [hep-ph].
- [11] K. T. Matchev and M. Park, arXiv:0910.1584 [hep-ph].
- [12] H. C. Cheng and Z. Han, JHEP **0812**, 063 (2008).
- [13] G. L. Bayatian *et al.*, J. Phys. G **34**, 995 (2007).
- [14] T. Sjostrand, S. Mrenna and P. Skands, JHEP **0605**, 026 (2006).
- [15] <http://www.physics.ucdavis.edu/~conway/research/>
- software/pgs/pgs4-general.htm
- [16] Yu. Pakhotin *et al.*, CERN-CMS-NOTE-2006-134.
- [17] The measured value of $M_{T2\perp}^{max}$ in Fig. 3 already implies that the mass splitting $M_p - M_c$ is on the order of 30 GeV, resulting in a rather soft lepton p_T spectrum.
- [18] The corresponding analytical results for $M_{T2\parallel}$ can be found in the first version of this paper, which is available on the hep-ph archive.